Spectrochimica Acta Part A: Molecular and Biomolecular Spectroscopy 122 (2014) 365–374

Contents lists available at ScienceDirect

Spectrochimica Acta Part A: Molecular and Biomolecular Spectroscopy

journal homepage: www.elsevier.com/locate/saa

Synthesis of mononuclear copper(II) complexes of acyclic Schiff's base ligands: Spectral, structural, electrochemical, antibacterial, DNA binding and cleavage activity

Arumugam Jayamani [a], Vijayan Thamilarasan [a], Nallathambi Sengottuvelan [a,*], Paramasivam Manisankar [b], Sung Kwon Kang [c], Young-Inn Kim [d], Vengatesan Ganesan [e]

[a] DDE, Alagappa University, Karaikudi 630 003, India
[b] Department of Industrial Chemistry, Alagappa University, Karaikudi 630 003, India
[c] Department of Chemistry, Chungnam National University, Daejeon 305-764, Republic of Korea
[d] Department of Chemistry Education and Interdisciplinary Program of Advanced Information and Display Materials, Pusan National University, Pusan 609-735, Republic of Korea
[e] AcmeProGen Biotech (India) Pvt. Ltd., Salem 636 004, India

HIGHLIGHTS

- Mononuclear Cu(II) complexes were synthesized using Schiff's base acyclic ligands.
- Single crystals X-ray study confirms the structure of ligands L^1 and L^2.
- Cu(II) ion in complexes was translocated between two non-equivalent compartments.
- All complexes show efficient DNA binding and cleavage ability.
- Oxidative cleavage mechanism using singlet oxygen as reactive species.

GRAPHICAL ABSTRACT

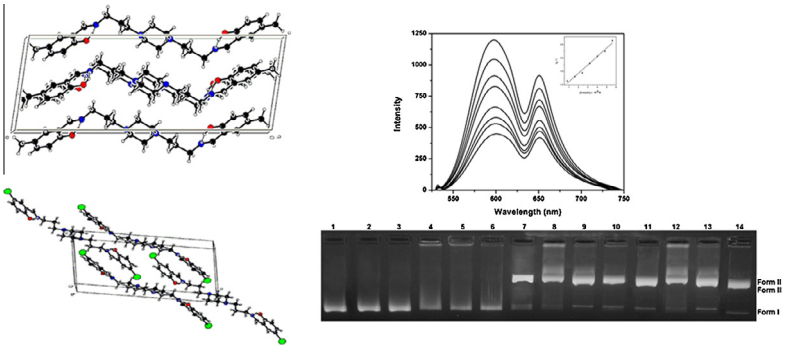

ARTICLE INFO

Article history:
Received 29 July 2013
Received in revised form 7 November 2013
Accepted 13 November 2013
Available online 21 November 2013

Keywords:
Copper(II) complexes
Acyclic Schiff's base
Anti bacterial activity
DNA binding and cleavage studies
Electrochemical studies

ABSTRACT

The mononuclear copper(II) complexes (**1**&**2**) of ligands L^1 [N,N′-bis(2-hydroxy-5-methylbenzyl)-1,4-bis(3-iminopropyl)piperazine] or L^2 [N,N′-bis(2-hydroxy-5-bromobenzyl)-1,4-bis(3-iminopropyl) piperazine] have been synthesized and characterised. The single crystal X-ray study had shown that ligands L^1 and L^2 crystallize in a monoclinic crystal system with $P2_1/c$ space group. The mononuclear copper(II) complexes show one quasireversible cyclic voltammetric response near cathodic region (−0.77 to −0.85 V) in DMF assignable to the Cu(II)/Cu(I) couple. Binding interaction of the complexes with calf thymus DNA (CT DNA) investigated by absorption studies and fluorescence spectral studies show good binding affinity to CT DNA, which imply both the copper(II) complexes can strongly interact with DNA efficiently. The copper(II) complexes showed efficient oxidative cleavage of plasmid pBR322 DNA in the presence of 3-mercaptopropionic acid as reducing agent through a mechanistic pathway involving formation of singlet oxygen as the reactive species. The Schiff bases and their Cu(II) complexes have been screened for antibacterial activities which indicates that the complexes exhibited higher antimicrobial activity than the free ligands.

Introduction

The developments of compounds cleaving DNA under physiological conditions is of current interest, due to their potential applications in genomic research and as foot printing and

* Corresponding author. Tel./fax: +91 9488260744.
E-mail address: nsvelan1975@yahoo.com (N. Sengottuvelan).

1386-1425/$ - see front matter © 2013 Elsevier B.V. All rights reserved.
http://dx.doi.org/10.1016/j.saa.2013.11.079

therapeutic agents [1–3]. Transition metal complexes have been widely exploited for metallohydrolases capable of mimicking the function of endonucleases [4] and to develop synthetic binding and cleavage agents for DNA. Especially, copper(II) complexes with Schiff's base ligands have been extensively explored in virtue of their strong interactions with DNA via surface associations or intercalation [5] and potential DNA cleavage activities via hydrolytic or oxidative mechanisms [6]. Copper(II) complexes are regarded as the most promising alternatives to cis-platin as anticancer drugs. The stability and functionality of the Schiff's base complexes were enhanced when the ligand molecules has controllable molecular motions. The controllable molecular motion can be induced by variation of a bulk parameter, such as the pH or the redox potential [7]. Transition metal ions can be translocated between two non-equivalent coordinating compartments of a ditopic ligand by varying the pH or redox potential. Enzymes such as haemocyanin [8] or tyrosinase [9] have a binuclear copper centre in their active sites. The geometry, the coordination sites, the bridging ligands between the centre, etc., define the properties of the binuclear centres Several metal complexes of Schiff bases derived from salicylaldehyde and amines [10,11] were reported and some of them have been proven to be efficient DNA cleavers [12,13] and as novel tumour chemotherapeutic and radio imaging agents [14].

In this work, we have been studying the DNA binding and cleavage activity of two new copper(II) complexes of ligands L^1 and L^2. The piperazine-imine-phenol Schiff base ligands L^1 and L^2 have been chosen considering that the phenolic –OH group may enhance the affinity of the complexes towards DNA binding through formation of hydrogen bonding.

Herein we report synthesis, characterisation, DNA binding and cleavage properties of copper(II) complexes (**1**&**2**). The ligands L^1 and L^2 have been structurally characterised by X-ray crystallography. The redox activity of complexes was evaluated by cyclic voltammetry. The DNA binding and cleavage ability of all the copper(II) complexes were evaluated using calf thymus and plasmid pBR322 DNA respectively. The antimicrobial property of ligands and their complexes were also assessed with two gram negative and two gram positive bacterium.

Experimental

Materials and instruments

All the chemicals used were of analytical grade and were used as received without any further purification. All the solvents were purified according to standard procedures. CT DNA and pBR322 DNA were purchased from SRL (India), Tris–HCl, Trisbase and NaCl were purchased from Merck. Double distilled water was used to prepare all buffer solutions.

The electronic spectra were recorded on a Shimadzu UV-3101PC spectrophotometer. FT-IR spectra were recorded in the 4000–400 cm^{-1} region using KBr pellets on a Bruker EQUINOX 55 spectrometer. The ^1H NMR spectrum of ligands were recorded in $CDCl_3$ on a BRUKER 300 MHz spectrometer at room temperature using TMS as an internal reference. Elemental analysis was carried out on an Elementarvario MACRO cube elemental analyzer. The EPR spectra were recorded at room temperature with a Bruker ESP 300E X-band spectrometer operating at 100 kHz. ESI mass spectra was obtained from Agilent 6520 Q-T mass spectrometer (CDRI, Lucknow, India). A Biologic CHI604D electrochemical analyzer was used for studying the electrochemical behaviour of complexes using a three-electrode cell in which a glassy carbon electrode was the working electrode, a saturated Ag/AgCl electrode was the reference electrode and a platinum wire was used as an auxiliary electrode in nitrogen atmosphere. The concentration of complexes was 10^{-3} M in DMF and tetra(n-butyl)ammonium perchlorate (TBAP) (10^{-1} M) was used as the supporting electrolyte.

Spectrophotometric titrations were performed on aqueous solutions (10 mL, made 0.05 M in $NaClO_4$, 25 °C) of the metal complexes at approximately adjusted pH of 2.0 by adding small amounts of a standard solution of $HClO_4$. Subsequently, additions of standard solutions (0.1 M) of NaOH were made until a basic pH (~12.0) was attained. Absorption spectra were taken after each addition of base. In each experiment the overall addition was limited to about 200 μl, so that volume variation was not significant. Safety note; Perchlorate salts of metal complexes are potentially explosive and should be handled with care.

Synthesis of ligands and complexes

Synthesis of ligand L^1

A methanolic (10 mL) solution of 5-methylsalicylaldehyde (2.2 mM, 0.30 g) was mixed with 1, 4-bis (3-aminopropyl) piperazine (2.2 mM, 0.44 g) dissolved in methanol (10 mL). The mixture was stirred for 30 min at room temperature to give a clear yellow solution. Then the content was refluxed for about 3 h. Yellow rod-shaped crystals were formed at the bottom of the vessel by slow evaporation of the solvent. The crystals were isolated by filtration, washed with methanol and dried. Yield: 0.64 g (87%) m.p.: 102 °C. Anal. Calcd. (%) for $C_{26}H_{36}N_4O_2$: C, 71.53; H, 8.31; N, 12.83. Found (%): C, 71.02; H, 8.76; N, 12.75. FT-IR, (ν, cm^{-1}) (KBr Disc): 3450br, 3012s, 2863s, 2932w, 2979br, 1133s, 1637s (br, broad; s, sharp; m, medium; w, weak). ^1H NMR, (300 MHz, $CDCl_3$): δ = 12.78 (Ar-OH, 2H); 8.29 (CH, 2H); 7.32–6.80 (- ArH, 6H); 2.39-3.55(-CH_2, 12H); 2.35(-CH_3, 6H); 1.82-1.88 (-CH_2, 8H). λ_{max}, nm (ε, M^{-1} cm^{-1}) in DMF: 325 (13,200), 270 (14,900).

Synthesis of ligand L^2

Ligand L^2 was synthesised using the same procedure as L^1 using 5-bromosalicylaldehyde (2.2 mM, 0.40 g) instead of 5-methylsalicylaldehyde. Yellowish orange, rod-shaped crystals were obtained at the bottom of the vessel. The crystals were isolated by filtration, washed with methanol and dried. Yield: 0.70 g (82%) m.p.: 125 °C. Anal.Calcd. (%) for $C_{24}H_{30}Br_2N_4O_2$: C, 50.90; H, 5.34; N, 9.89. Found (%): C, 50.82; H, 5.76; N, 9.75. FT-IR (ν, cm^{-1}) (KBr Disc): 3423br, 3000w, 2857br, 2939s, 1128s, 1628s. ^1H NMR (300 MHz, $CDCl_3$): δ = 12.96 (Ar-OH, 2H); 8.19 (CH, 2H); 7.32–6.82(ArH, 6H); 2.39–2.42 (CH_2, 12H); 1.86 (CH_2, 8H). λ_{max}, nm (ε, M^{-1} cm^{-1}) in DMF: 328 (14,200), 272 (15,600).

Synthesis of copper(II) complexes

$[CuL^1](ClO_4)_2$(1). To a solution of ligand (L^1) (0.20 g, 0.46 mM) in methanol (10 mL), $Cu(ClO_4)_2.6H_2O$ (0.17 g, 0.46 mM) in 10 mL of methanol was added drop wise. The mixture was stirred well at room temperature and the content was refluxed for about 2 h. The resultant dark green solution was then concentrated to one third of its volume and washed well with water, ethanol and ether and dried under vacuum. Yield: 0.27 g (74%). m.p.: 174 °C (dec.). Anal. Calc. (%) for $C_{26}H_{36}Cl_2CuN_4O_{10}$: C, 44.67; H, 5.19; N, 8.01; Cu, 9.09. Found (%): C, 44.47; H, 5.04; N, 8.08; Cu, 8.95. FT-IR (ν, cm^{-1}) (KBr Disc): 3450w, 3010s, 2867 m, 2923br, 1630s, 1139s, 625w. λ_{max}, nm (ε, M^{-1} cm^{-1}) in DMF: 568 (520), 383 (13,900), 286 (99,200); Conductance (Λ_m/S cm^2 mol^{-1}) in acetonitrile 165. $g_{||}$ = 2.14, $g_{\perp}$ = 2.08, and $A_{||}$ = 324; ESI-MS in CH_3CN *m/z* (%): 380.3 (9) $[C_{26}H_{36}N_4O_2]^+$, 498.3 (100) $[CuL^1]^+$, 696.2(2) $[CuL^1 + 2ClO_4]^+$.

$[CuL^2](ClO_4)_2$(2). The complex **2** was synthesised using the same procedure as **1** using ligand L^2(0.20 g, 0.35 mM) instead of L^1 with $Cu(ClO_4)_2.6H_2O$ (0.13 g, 0.35 mM) in 10 mL of methanol. Yield: 0.23 g (70%). m.p.: 210 °C (dec.). Anal. Calc. (%) for $C_{24}H_{30}Br_2Cl_2$

CuN_4O_{10}: C, 34.78; H, 3.65; N, 6.76; Cu, 7.67. Found (%): C, 34.56; H, 3.76; N, 6.86; Cu, 7.95. FT-IR (ν, cm^{-1}) (KBr Disc): 3425br, 3017 m, 2881 m, 2958s, 1625s, 626w. λ_{max}, nm (ε, M^{-1} cm^{-1}) in DMF: 571 (1400), 382 (17,300), 287 (99,900); Conductance (Λ_m/S cm^2 mol^{-1}) in acetonitrile 172. $g_{||}$ = 2.14, $g_{\perp}$ = 1.88 and $A_{||}$ = 358.

X-ray diffraction analysis

Yellow crystals of the ligands L^1 and L^2 suitable for X-ray diffraction studies were obtained from slow evaporation of chloroform solution, after standing for two days. The X-ray diffraction analysis of the ligands was performed on Bruker SMART APEX-II CCD diffractometer using graphite monochromated Mo Kα radiation (0.71037 Å). The structure was solved using the direct methods and successive Fourier difference synthesis thermal parameters for all non-hydrogen atoms (SHELXL-97) and all non-hydrogen atoms were refined anisotrophically by full-matrix least-square procedures. Hydrogen atoms were added theoretically and refined with riding model position parameters and fixed isotropic thermal parameters.

DNA binding and cleavage studies

The binding of CT DNA with copper(II) complexes were studied using the UV absorption spectral method. Solutions of CT DNA in 50 mM NaCl/5 mM Tris–HCl (pH = 7.4) gave a ratio of A_{260}/A_{280} as 1.8–1.9, indicating that the DNA was sufficiently free of protein contamination. The DNA concentration was determined by the UV absorbance at 260 nm after 1:100 dilutions. The molar absorption coefficient was taken as 6600 M^{-1} cm^{-1} [15]. Stock solutions were stored at 4 °C and used within Four days. Absorption titration experiments were made using different concentration of DNA, while keeping the complex concentration as constant.

No luminescence was observed for complexes **1**&**2** at room temperature in aqueous solution, in any organic solvent examined, or in the presence of CT-DNA. So the binding of complexes cannot be directly presented in the emission spectra. Therefore, the fluorescence spectral method, using ethidium bromide (EB) as a reference was used to determine the relative DNA binding properties of complexes **1**&**2** to CT DNA in 5 mM Tris–HCl/5 mM NaCl buffer, pH 7.2. Fluorescence intensities of EB at 600 nm with an excitation wavelength of 515 nm were measured at different complex concentrations. Reduction in the emission intensity was observed with addition of the complexes. The relative binding tendency of the complexes to CT DNA was determined from a comparison of the slopes of the lines in the fluorescence intensity versus complex concentration plot. The apparent binding constant (K_{app}) was calculated using the equation K_{EB}/[EB] = K_{app}[Complex], where the complex concentration equalled the value at a 50% reduction of the fluorescence intensity of EB and $K_{EB} = 1.0 \times 10^7$ M^{-1} ([EB] = 3.3 μM).

The DNA cleavage studies were done by gel electrophoresis experiment for which pBR322 was used as the plasmid DNA. DNA cleavage activity was evaluated by monitoring the conversion of supercoiled plasmid DNA (Sc – form I) to nicked circular DNA (Nick-form II) and linear DNA (Lin – form III). Each reaction mixture was prepared by adding 6 μL of water, 2 μL (200 ng) of supercoiled DNA, 2 μL of 500 mM Tris–HCl/500 mM NaCl buffer (pH = 7.4), 4 μL of 3-mercaptopropionic acid 6 μL of the complex dissolved in DMF. The final reaction volume was 20 μL, the final buffer concentration was 50 mM and the final metal concentration varied from 100 to 200 μM. For investigation of the mechanistic aspects, the cleavage of pBR322 DNA was also carried out in the presence of standard hydroxyl radical scavenger such as DMSO and KI, and singlet oxygen ($^1O_2$) quencher such as L-histidine and NaN_3. Samples were typically incubated for 1 h at 37 °C. After incubation, 5 μL of DNA loading buffer (0.25% bromophenol blue, 0.25% xylene cyanol, 30% glycerol in water) were added to each tube and the sample was loaded onto a 0.8% agarose gel in TBE buffer (89 mM Tris–borate, 1 mM EDTA pH8.4) containing ethidium bromide (0.5 μg/mL). Negative and positive controls were loaded on each gel electrophoresis and the experiment was carried out for 1.30 h at 50 V.

Antibacterial screening

Antibacterial activity of the ligands and their complexes were tested against the bacterial species *Staphylococcus aureus*, *Escherichia coli*, *Bacillus subtlis*, *Pseudomonas aeruginosa* by disc diffusion method using nutrient agar medium. Nutrient agar (20 mL) were poured into each sterilized Petri dish (10 × 100 mm diameter) and allowed to solidify. After solidification the bacterial culture were swabbed in nutrient agar plates. For the investigation of the antibacterial activity, the ligands and their copper complexes were dissolved in dimethylsulfoxide (DMSO) to a final concentration of 100 μg/mL. Each sample was filled into the Sterilized discs of agar plates directly. Plates swabbed with the bacteria culture were incubated at 37 °C for 18 h. At the end of the incubation period, inhibition zones formed on the medium were evaluated in mm and studies were performed in duplicate. Solvent control test was also performed in order to study the effect of DMSO (solvent) on the growth of microorganism and it did not inhibit growth.

Results and discussion

Synthesis and characterization

The synthesis of the Cu(II) complexes with the ligands of the Schiff base type were done using a common procedure, by reaction of stoichiometric amount of copper perchlorate salts with the

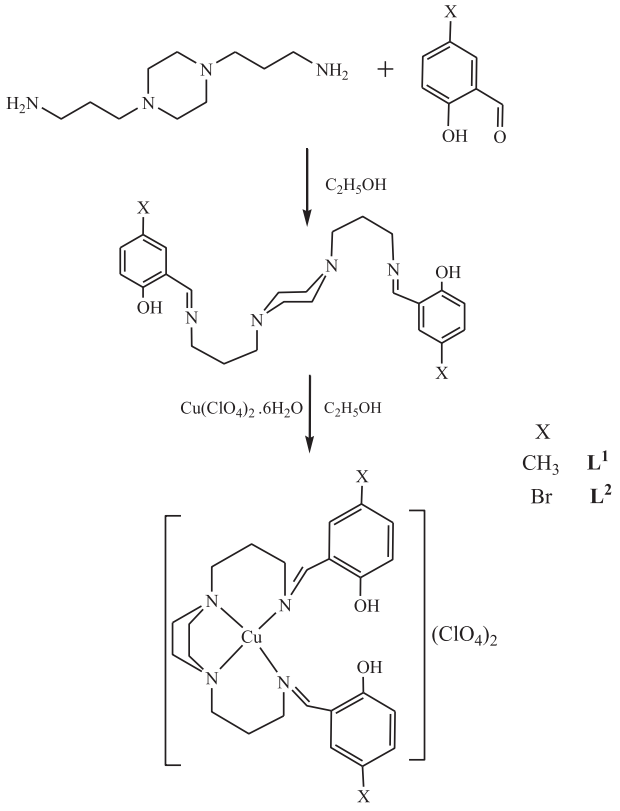

Scheme 1.

ligands in methanol as given in the Scheme 1. The analytical data obtained for complexes **1**&**2** are consistent with the formation of mononuclear copper complexes. The obtained complexes are insoluble in water, methanol, ethanol, and chloroform but soluble in acetonitrile, Dimethylformamide (DMF) and DMSO.

X-ray crystal studies

The crystals of ligands L^1 and L^2 were obtained by slow evaporation method using chloroform as solvent were shown in Fig. 1. The details of the crystal data and refinement for L^1 and L^2 were given in Table 1, selected bond lengths and angles are listed in Table 2. Both the crystals, crystallizes in the monoclinic crystal system with space group $P2_1/c$ with molecular formulae $C_{26}H_{36}N_4O_2$ (L^1) and $C_{24}H_{30}Br_2N_4O_2$ (L^2). As depicted in Fig. 1(a) and (b), the L^1 and L^2 contain one crystallographically unique piperazine ring and two 5-methyl salicylaldehyde and 5-bromosalicylaldehyde respectively. The piperazine ring of the ligands can be regarded as three moieties: plane A composed of N(14A)–C(15A)–C(16), ring B composed of C(15)–C(16)–C(15A)–C(16A), and plane C composed of N(14)–C(15)–C(16A) for both the ligands. The atoms of ring B are perfectly coplanar for the mean deviation from the plan is 0.0000 Å, and N(14) atom and N(14A) atom lies above or below the plan by −1.458 and 1.458 Å for L^1 and by −1.456 and 1.456 Å for L^2 with respect to one another. Furthermore the dihedral angle between the plane A and B is 57.6° for L^1 and 57.8° for L^2, equal to that of B and C for both ligands respectively, and that of A and C is 0° for both ligands. Therefore, plane A and C parallel to each other, indicating that the piperazine ring in both the ligands adopts the stable chair conformation, not the boat conformation [16].

The bond length of azomethine C9=N10 Å in L^1 and L^2 were consistent with normal C=N bond lengths [17]. The bond angle of C(13)N(14)C(15) was found to be 110° but the bond angle of C(9)N(10)C(11) bond angle at 119.6° which clearly indicates the formation of C=N bond confirming the formation of Schiff's base in both ligands. In the crystal structure of L^1 the 5-methylsalicylaldehyde group is in the same plane of piperazine unit with torsion angle of 179.89° in the place of azomethine group, but in case of L^2 5-bromosalicylaldehyde is not parallel to piperazine moiety, it has the torrision angle of 178.18° in the place of azomethine group. The difference between both the structures may be attributed due to the presence of electron withdrawing bromine atom in L^2.

The packing of the L^1 and L^2 in the unit cell showing the intermolecular and intramolecular interactions were depicted in Fig. 2. An intramolecular hydrogen bonding O_7–$H_7\cdots N_{10}$ at a bond distance of 2.594 Å for L^1 and O_8–$H_8\cdots N_{10}$ for L^2 at a bond distance of 2.575 Å, linking the OH group of the former salicylaldehyde and the imine N atom of amine stabilises the molecule. In addition, the L^1 is further connected by C_8–$H_{8c}\cdots H_{8c}$ at a bond distance of 2.399 Å with another molecule (hydrogen bonds) forming one dimensional infinite chain which stabilises the crystal packing. In case of L^2 there are four intermolecular interactions noted at $Br_7\cdots N_{14}$ (3.21 Å), $Br_7\cdots H_{11B}$ (2.999 Å), C_2-$H_2\cdots H_2$ (2.352 Å) and O_8-$H_8\cdots H_{13A}$ (2.622 Å) stabilises the crystal packing. The packing is further stabilized by Vander Waals interactions.

Spectral characterization

The FT-IR spectrum of ligands showed the band at 1281 cm^{-1} associated with phenolic ν(C-O) stretching frequency and the broad peak at 3423–3450 cm^{-1} is assigned to the phenolic ν(OH) group. The ligands and complexes show a sharp band in the region of 1620–1650 cm^{-1} due to thepresence of ν(C=N) in the ligand and in complexes [18]. The effective Schiff base condensation is confirmed by the formation of this new peak and the disappearance of the ν(C=O) peak at 1680 cm^{-1} in the reactant molecule (5-methyl salicylaldehyde). Both the copper(II) complexes showed a strong band around 1000–1100 cm^{-1} and a sharp band in the region around 625 cm^{-1} due to the antisymmetric stretch and antisymmetric bend of the perchlorate ions, respectively. No splitting of the perchlorate peak indicates that the perchlorate ions are not coordinated to the Cu(II) ions and are present as counter ions in crystal lattice [19,20]. Conductivity measurement of mononuclear copper(II) complexes in acetonitrile are in the range of 165–172 Λ_m/S cm^2 mol^{-1} indicates that the complex is 1:2 electrolyte type [21].

The absorption spectral data for Schiff's base ligands and their complexes were obtained in DMF solution. In the UV region, band at 325 nm (13,200 cm^{-1}) for L^1 and 328 nm (14,200 cm^{-1}) for L^2 are due to the $n \rightarrow \pi^*$ transition of azo-methine (C=N) function of Schiff's base and the band at 270 nm (14,900 M^{-1} cm^{-1}) for L^1 and at 272 nm (15,600 M^{-1} cm^{-1}) for L^2 are due to $\pi \rightarrow \pi^*$ of the aromatic moiety in ligands. In case of complexes, the peaks in the region of 286 and 289 nm are obtained due to $\pi \rightarrow \pi^*$ transition of coordinated ligands. In the UV region of complexes show broad, slightly intense bands between 382 and 383 nm could be assigned to ligand to metal charge transfer transition [22]. In the visible region of both complexes the broad absorption band at about 568–571 nm, which is assigned to a d–d transition, which is consistent with the square-planar geometry of the Cu(II) complexes. For

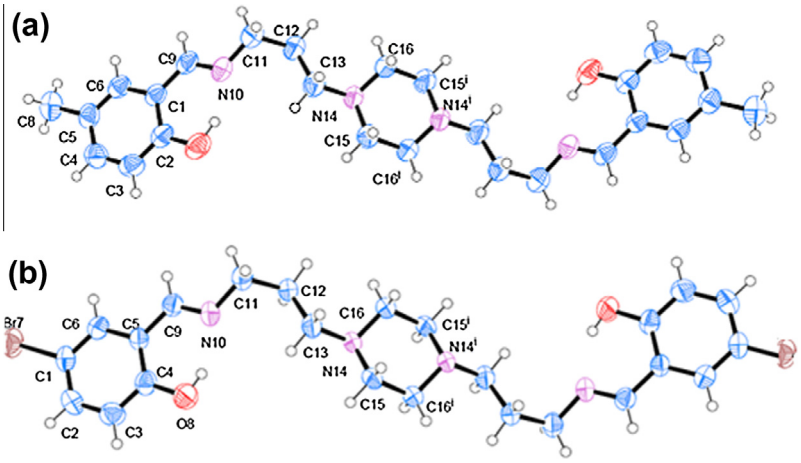

Fig. 1. OPTEP view of the molecular structure and atom labeling scheme of L^1 (a) and L^2 (b).

Table 1
Crystallographic data & structure refinement parameters for ligands L^1 and L^2.

	L^1	L^2
Empirical formula	C_{26} H_{36} N_4 O_2	C_{24} H_{30} Br_2 N_4 O_2
Formula weight	436.59	566.34
Temperature (K)	296(2)	296(2)
Wavelength (Å)	0.71073	0.71073
Crystal system, space group	Monoclinic, $P2_1/c$	Monoclinic, $P2_1/c$
a (Å)	23.952(7)	10.0467(2)
B (Å)	5.8556(14)	6.54420(10)
c (Å)	8.969(3)	19.1166(3)
α (°)	90	90
β (°)	98.727(16)	102.1260(10)
γ (°)	90	90
Volume (Å^3)	1243.3(6)	1228.94(4)
Z, calculated density (mg m^{-3})	2, 1.166	2, 1.530
Absorption coefficient (mm^{-1})	0.075	3.326
F(000)	472	576
Crystal size (mm)	0.32 × 0.30 × 0.11	0.17 × 0.15 × 0.14
Theta range for data collection (°)	0.86–25.49	2.07–28.30
Limiting indices, *h*, *k*, *l*	$-26 \leqslant h \leqslant 27$, $-7 \leqslant k \leqslant 4$, $-10 \leqslant l \leqslant 8$	$-13 \leqslant h \leqslant 13$, $-8 \leqslant k \leqslant 8$, $-25 \leqslant l \leqslant 25$
Reflections collected/unique	9411/2240	27402/3051
R int	0.1133	0.0814
Data/restraints/parameters	2240/0/150	3051/0/149
Goodness-of-fit on F^2	1.064	0.812
Final *R* indices [$I > 2\sigma$ (*I*)]	R1 = 0.0626, wR2 = 0.1813	R1 = 0.0300, wR2 = 0.0574
R indices (all data)	R1 = 0.1050, wR2 = 0.2451	R1 = 0.0694, wR2 = 0.0639
Largest difference peak and hole/e Å^{-3}	0.213 and −0.283	0.214 and −0.363

Table 2
Selected bond lengths (Å) and bond angles (°) for L^1 and L^2.

Ligand L^1				Ligand L^2			
Bond distances (Å)		Bond angles (°)		Bond distances (Å)		Bond angles (°)	
C(1)–C(9)	1.460(4)	C(6)–C(1)–C(2)	118.5(3)	C(1)–Br(7)	1.902(2)	C(6)–C(1)–C(2)	120.0(2)
C(2)–O(7)	1.345(3)	C(6)–C(1)–C(9)	120.9 (2)	C(4)–O(8)	1.350(3)	C(6)–C(1)–Br(7)	119.47(18)
O(7)–H(7)	0.940(4)	C(2)–C(1)–C(9)	120.6(2)	O(8)–H(8)	0.82(2)	C(2)–C(1)–Br(7)	120.48(18)
N(10)–C(11)	1.461(4)	O(7)–C(2)–C(3)	120.0(2)	N(10)–C(11)	1.462(3)	O(8)–C(4)–C(3)	118.4(2)
N(14)–C(15)	1.458(3)	O(7)–C(2)–C(1)	121.3(3)	N(14)–C(15)	1.456(2)	O(8)–C(4)–C(5)	121.8(2)
C(2)–C(3)	1.383(4)	C(6)–C(5)–C(8)	121.8(3)	C(2)–C(3)	1.375(3)	C(6)–C(5)–C(9)	120.51(19)
C(5)–C(8)	1.502(4)	C(2)–O(7)–H(7)	109.0(3)	C(5)–C(9)	1.458(3)	C(4)–O(8)–H(8)	105.2(19)
C(9)–N(10)	1.261(3)	N(10)–C(9)–C(1)	122.4(2)	C(9)–N(10)	1.267(3)	N(10)–C(9)–C(5)	121.7(2)
C(13)–N(14)	1.452(3)	C(9)–N(10)–C(11)	119.6(2)	C(13)–N(14)	1.465(2)	C(9)–N(10)–C(11)	118.93(19)
N(14)–C(15)	1.458(3)	N(10)–C(11)–C(12)	112.3(2)	N(14)–C(16)	1.458(2)	N(10)–C(11)–C(12)	111.50(18)
		N(14)–C(13)–C(12)	114.2(2)			N(14)–C(13)–C(12)	114.19(17)
		C(16)–N(14)–C(15)	108.0(2)			C(15)–N(14)–C(16)	108.37(16)
		N(14)–C(15)–C(16)#1	111.7(2)			N(14)–C(15)–C(16)#1	111.50(17)
		N(14)–C(16)–C(15)#1	111.0(2)			N(14)–C(16)–C(15)#1	110.53(17)

square planar complexes with d_{x2-y2} ground state, three spin allowed transitions are possible viz., $^2B_{1g} \rightarrow {}^2A_{1g}$ ($d_{x2-y2} \rightarrow d_{z2}$), $^2B_{1g} \rightarrow {}^2B_{2g}$ ($d_{x2-y2} \rightarrow d_{xy}$) and $^2B_{1g} \rightarrow {}^2E_g$ ($d_{x2-y2} \rightarrow d_{xz}$, d_{yz}) but it is often difficult to resolve into three bands since the four lower orbitals are so close together in energy that individual transfer from these to the upper d level cannot be distinguished. The third peak in the wavelength range 568–571 nm corresponds to d–d transition of this type as expected for square planar copper(II) complexes [23–25]. Therefore, it appears that there is a distorted square-planar geometry of the Cu centers in the copper(II) complexes.

Electron Spray Ionization (ESI) mass data of **1** shows the molecular ion peak at *m*/*z* 696.2(2) which is assignable to $[CuL^1 + 2ClO_4]^+$ and the loss of perchlorate ions forms a base peak at *m*/*z* 498.3(100) due to the formation of $(CuL^1]^+$. Few other intense peaks are also obtained for **1** at *m*/*z* 380.3, 249.8, and 211.2. The mass spectra of mononuclear copper(II) complexes 1 was displayed in Fig. S1. The ESI mass spectral data of the Schiff base copper(II) complexes are in good agreement with the proposed structure of mononuclear copper(II) complexes.

pH-controlled complexation–decomplexation

The solution of 0.05 M in sodium perchlorate of the mononuclear copper(II) complexes was acidified to pH 2 and was titrated with standard NaOH. The titration curve disclosed a single deprotonation event, with a $pK_a = 7.85 \pm 0.05$, to be ascribed to the acid–base equilibrium. Titration with base induces decolorisation of the blue to green solution and a considerable change of the absorption spectrum, as shown in Fig. 3. In particular, the strong band at 389 nm (ε – 8870 M^{-1} cm^{-1}) decreases, while a new band develops at 338 nm (ε – 6750 M^{-1} cm^{-1}, limit value at pH 12) for $[CuL^1]$ complex. In case of $[CuL^2]$ complex, the strong band at 387 nm (ε – 7487 M^{-1} cm^{-1}) decreases, while a new band develops at 336 nm (ε – 5348 M^{-1} cm^{-1}, limit value at pH 12). Quite interestingly, on increasing pH the molar absorbance of the new band superimposes well with the concentration profile of the $[Cu^{II}(L)]^+$ species, as shown in Fig. 3(a) and (b). The shift of the wavelength in the visible region from 560-570 nm to 590-600 nm on varying the pH (acidic to basic) of the mononuclear copper(II) complexes indicates that the colour and spectral changes are associated to

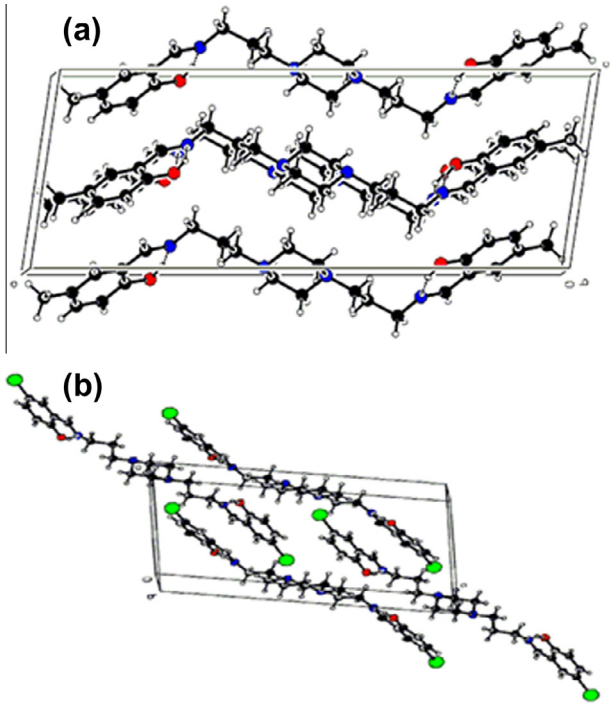

Fig. 2. Crystal packing diagram of L^1 (a) and L^2 (b).

the deprotonation process and thus the molecular motion [7] i.e. the change of the position of copper atom from N_4 compartment to N_2O_2 compartment, is achieved on varying the pH of the complex solution.

Electrochemical studies

The electrochemical behaviour of the complexes have been studied using cyclic voltammetry in the potential range of 0 to −1.80 V in dimethylformamide containing 10^{-1} M tetra(n-butyl)ammonium perchlorate. The voltammetric data are summarized in Table 3. Cyclic voltammograms for all the complexes (scan rate 50 mV s^{-1}) were displayed in Fig. 4. Controlled potential electrolysis performed at a potential 100 mV morenegative than the reduction wave indicates the consumption of one electron per molecule for both the first and second reduction wave.

Table 3
Electrochemical data of mononuclear copper (II) complexes.

Complexes	E^1_{pc}	E^1_{pa}	$E^1_{1/2}$	ΔE^1
$[CuL^1](ClO_4)_2$	−0.85	−0.51	−0.68	340
$[CuL^2](ClO_4)_2$	−0.77	−0.49	−0.63	280

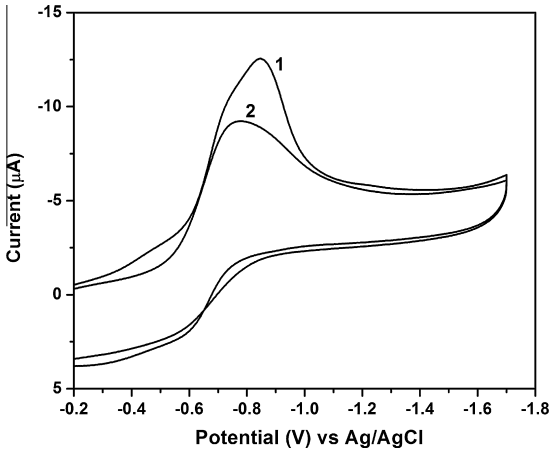

Fig. 4. Cyclic voltammogram of the mononuclear copper(II) complexes. (**1**) $[CuL^1](ClO_4)_2$, (**2**) $[CuL^2](ClO_4)_2$ (Reduction process).

The mononuclear complex **1** shows one quasi-reversible reduction wave (E^1_{pc} = −0.85 V and E^1_{pa} = −0.51 V) in the cathodic potential at $E_{1/2}$ = −0.68 V versus Ag/AgCl and the complex **2** shows a quasi-reversible reduction wave (E^1_{pc} = −0.77 V and E^1_{pa} = −0.49 V) in the cathodic potential at $E_{1/2}$ = −0.63 V versus Ag/AgCl. The potentials at the reduction wave of the $[CuL^2](ClO_4)_2$ was lower than that of $[CuL^1](ClO_4)_2$ is due to the electron-withdrawing bromide ion that is present at the para position to the phenolic group which decreases the electron density at the metal centre leading to easy reduction, and shifts the reduction potential to less negative potential [26,27].

So the one redox couple of a single electron transfer for mononuclear complexes was assigned as,

$$Cu^{II} \rightleftharpoons Cu^{I}$$

Thus, the cavity of the complex easily holds the reduced cation and stabilizes the formation of Cu(I) in the compartment.

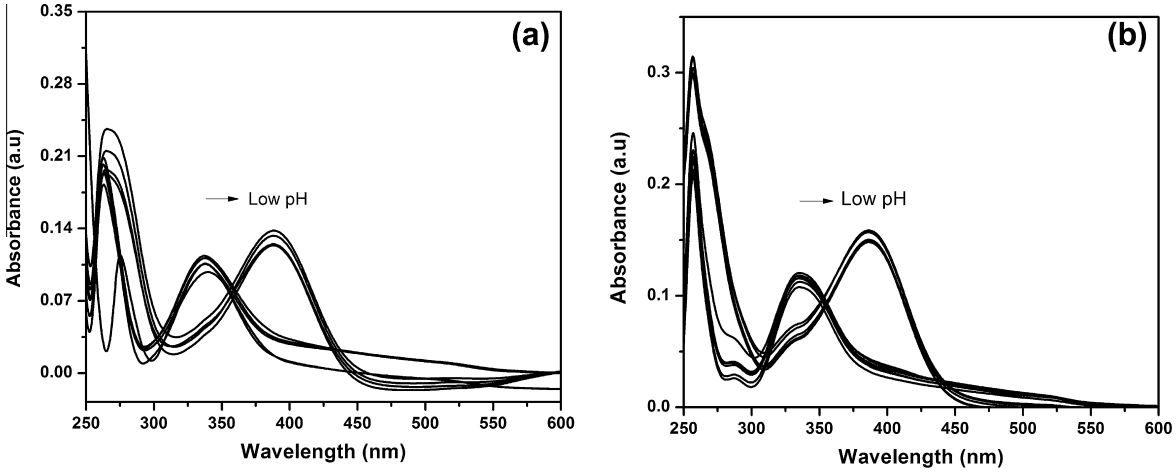

Fig. 3. Absorption spectra of **1** (a) and **2** (b) in water (10^{-5} M) measured during a titration with NaOH (pH range: 2–12).

ESR spectra

The ESR spectra of the mononuclear copper(II) complexes (**1**&**2**) show four lines with nuclear hyperfine spin 3/2 due to hyperfine splitting. For the mononuclear copper(II) complex **1**, the observed $g_{\perp}$, $g_{||}$ and $A_{||}$ values are 2.05, 2.14 and 324 respectively and for mononuclear copper(II) complex **2**, $g_{\perp}$, $g_{||}$ and $A_{||}$ values are 1.88, 2.14 and 358 respectively. The observed ESR spectral values are similar to a piperazine based mononuclear Cu(II) complex [28]. The fact that $g_{||} > g_{\perp}$, confirms a square planar geometry with a $(d_{x2-y2})^1$ as ground state in complexes **1**&**2**. For a Cu(II) complex, $g_{||}$ is a parameter sensitive enough to indicate covalence. The fact that $g_{||}$ less than 2.3 is an indication of significant covalent character to the M–L bond [29].

DNA binding studies

Absorption spectral studies

Absorption titration experiments were performed with fixed concentrations of the copper(II) complexes (40 μM) while gradually increasing the concentration of DNA (10 mM) at 25 °C. While measuring the absorption spectra, an equal amount of DNA was added to both the compound solution and the reference solution to eliminate the absorbance of DNA itself. We have determine the intrinsic binding constant to CT DNA by monitoring the absorption intensity of the charge transfer spectral bands near 260 and 275 nm for the complexes of [CuL^1] and [CuL^2], respectively.

Upon addition of increasing amount of CT DNA, a significant "hyperchromic" effect in the intraligand bands at 246–280 nm was observed accompanied by a moderate red shift of 2–3 nm, indicative of stabilization of the DNA helix. These spectral characteristic suggest that the complexes and ligand bind either to the external contact (electrostatic binding) or to the major and minor grooves of DNA. Moreover, this "hyperchromic effect" can be explained on the basis of two phenomena. Firstly, the large surface area of the ligand as well as presence of planar aromatic chromophore facilitates a strong binding interaction of the complexes with CT DNA there by, providing ample opportunity for the complex to bind with the CT DNA via, partial insertion of the aromatic moiety in between the stacking base pair. The binding interaction between the cationic complex and CT DNA leads to diffusion-limited ion-pair formation at higher concentration of the complex such that the complex is fitted along the contour of DNA double helix in an induced-fit fashion. Thus, the complexes preferably bind to the DNA helix via, groove binding interactions. This groove binding results in structural reorganization of CT DNA which entails partial unwinding or damage of the double helix at the exterior phosphate backbone leading to the formation of a cavity to accommodate the complex [30]. The spectrophotometric titration of the complex **1**&**2** are shown in Fig. 5. To compare quantitatively the binding strength of all the copper(II) complexes, the intrinsic binding constants K_b of all the complexes with CT DNA were determined according to the following equation [31].

$$[DNA]/(\varepsilon_a - \varepsilon_f) = [DNA]/(\varepsilon_b - \varepsilon_f) + 1/K_b(\varepsilon_b - \varepsilon_f)$$

where [DNA] is the concentration of DNA in base pairs, the apparent absorption coefficients ε_a, ε_f and ε_b correspond to $A_{obsd}/[Cu_2]$, the extinction coefficient for the free complexes and the extinction coefficient for the complexes in the fully bound form, respectively. In plots of $DNA]/(\varepsilon_b-\varepsilon_f)$ versus [DNA], K is given by the ratio of the slope to the intercept. The K_b values obtained from the absorption spectral technique for the complexes [CuL^1] and [CuL^2] were calculated as 4.89×10^5 and 7.89×10^5 M^{-1}, respectively. The binding constant of the copper(II) complexes of L^1 is comparatively lower than that of the copper(II) complexes of L^2, may be due to the presence of electron withdrawing group (Br) in L^2. Comparing the intrinsic binding constant of **1**&**2** with those of some other mono and binuclear Schiff base copper(II) complexes (Table 4), we conclude that these complexescan strongly bind to DNA and their binding constant is remarkable. Furthermore, the K_b values of **1**&**2** complexes are also higher than those of some other mononuclear Schiff's base copper(II) complexes as listed in Table 4 [32–37] and other well-established intercalation agents ($\approx 10^4$) [38–40]. This indicates that diverse bridging ligands have a profound effect on DNA-binding ability, as revealed by the different binding constants.

Fluorescence spectral studies

The fluorescence spectroscopy technique is an effective method to study metal complex interaction with DNA. The emission spectra of EB bound to DNA in the absence and presence of complexes **1**&**2** are shown in Fig. 6. The addition of the complex to DNA pretreated with EB causes an appreciable reduction in the fluorescence intensity, indicating that complexes **1**&**2** compete with EB to bind with DNA. The reduction of the emission intensity gives a measure of the DNA binding propensity of the complexes and stacking interaction between adjacent DNA base pairs [41]. According to the classical Stern–Volmer equation $I_0/I = 1 + K$ [Q]; I_0 and I are the fluorescence intensities in the absence and presence of the quencher, respectively; K is a linear Stern–Volmer quenching constant; [Q] is the concentration of the quencher. The fluorescence quenching curve of DNA-bound EB by complexes **1**&**2** illustrates that the quenching of EB bound to DNA by complexes **1**&**2** is in good agreement with the linear Stern–Volmer equation. In the linear fit plot of I_0/I versus [complex]/[DNA], K is given by the ratio of the slope to the intercept. The K values for complexes **1**&**2** are 1.25 ($R = 0.992$) and 1.65 ($R = 0.991$), respectively (I_0 is the emission intensity of EB-DNA in the absence of complex; I is the emission intensity of EB-DNA in the presence of complex). The apparent DNA binding constants (K_{app}) of 3.67×10^5 M^{-1} and 4.13×10^5 M^{-1} were derived {K_{EB}/([Complex]/[EB])} for complexes **1**&**2** respectively. The K_{app} values imply that all the complexes can strongly interact with DNA and are protected by DNA efficiently, since the hydrophobic environment inside the DNA helix reduces the accessibility of solvent water molecules to the complex and the complex's mobility is restricted at the binding site [42]. The presence of 5-methyl (or bromo)salicylaldehyde groups and also the hydrophobic property of the rigid ligand facilitate the DNA binding [43,44].

DNA cleavage studies

The DNA cleavage activity of complexes **1**&**2** have been studied by supercoiled pBR322 DNA as a substrate in a medium of 50 mM Tris–HCl/50 mM NaCl buffer (pH = 7.4) in the presence of mercaptopropionic acid as a reducing agent. When the original supercoiled form (Form I) of plasmid DNA is nicked, an open circular relaxed form (Form II) will exist in the system and the linear form (Form III) can be found upon further cleavage. During electrophoresis, the compact Form I migrates relatively faster while the nicked Form II migrates slowly, and the linearized form (Form III) migrates between Forms I and II.

Fig. 7 exhibits the results of the gel electrophoresis separations of plasmid pBR322 DNA by the complexes **1**&**2** in the presence of mercaptopropionic acid(MPA) which shows that the DNA cleavage of complexes **1**&**2** (lanes 3 and 4) have no conversion of supercoiled form to nicked form at 200 μM concentrations of complexes without the addition of reducing agent. But Form I (Super coiled DNA) was mostly converted to Form II (Nicked Circular DNA) at 100 μM concentration of the complexes **1**&**2** (lanes 5 and 6 respectively) in the presence of MPA. A minimum amount of DNA was completely cleaved to Form III (linear) as the concentration of complexes increased to 200 μM (lanes 7 and 8). The presence of

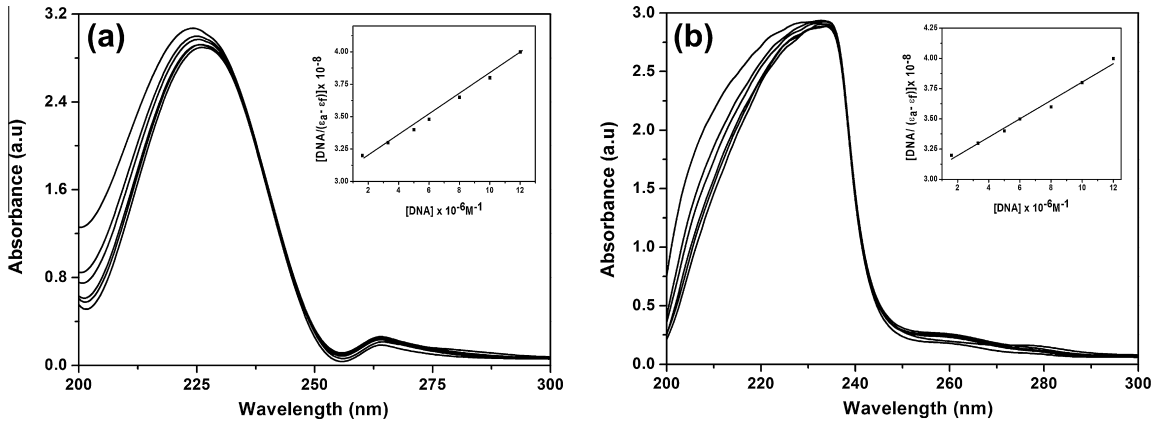

Fig. 5. Absorption spectra of (a) $[CuL^1](ClO_4)_2$ and (b) $[CuL^2](ClO_4)_2$(10^{-5} M) in 5 mM Tris–HCl/20 mM NaCl buffer at pH 7.2 in the absence and presence of increasing amounts of DNA.

Table 4
Intrinsic binding constants (K_b) and cleavage properties.

Compound	DNA binding constant K_b (mol $L^{-1})^{-1}$)	DNA cleavage studies	Reference
$[Cu(L^1)](ClO_4)_2$	4.89×10^5	Oxidative cleavage	This work
$[Cu(L^2)](ClO_4)_2$	7.89×10^5	Oxidative cleavage	This work
$[Cu_2(L^1)](ClO_4)_2$	8.02×10^5	Oxidative cleavage	This work
$[Cu_2(L^2)](ClO_4)_2$	1.09×10^4	Oxidative cleavage	This work
$[Cu(L^3)(phen)Cl]$	5.72×10^4	Notable cleavage	[32]
$[Cu(L^3)(bpy)Cl]$	1.55×10^4	Notable cleavage	[33]
$[Cu_2L^4(OAc)(CH_3OH)]\ CH_3OH$	1.16×10^5	Effective DNA-cleavage activity via hydrolytic-cleavage mechanism	[34]
$[Cu\ (L^5)]$	2.71×10^4	Moderate cleavage	[39]
$[CuL^6Cl_2]$	6.94×10^4	-	[35]
$[Cu(L^7)](ClO_4)_2$	8.56×10^4	Oxidative cleavage	[22]
$[Cu(L^8)](ClO_4)_2$	7.15×10^4	Oxidative cleavage	[22]
$[Cu(buobb)_2](pic)_2$	1.01×10^5	Oxidative cleavage	[36]
$[Cu_2L^9]$	2.76×10^5	Hydrolytic-cleavage	[37]
$[Cu_2L^{10}]$	6.07×10^5	Hydrolytic-cleavage	[37]

L^1 = N,N′-bis(2-hydroxy-5-methylbenzyl)-1,4-bis(3-iminopropyl)piperazine.
L^2 = N,N′-bis(2-hydroxy-5-bromobenzyl)-1,4-bis(3-iminopropyl)piperazine.
L^3 = Schiff's base formed from o-aminophenol and 2-methylacetoacetanilide.
L^4 = 1,3-bis (5-methylsalicylideneimino)propan-2-ol.
L^5 = Schiff's base formed from isatinmonohydrazone and 2,3,5-trichlorobenzaldehyde.
L^6 = Schiff's base formed from 5-nitro-o-vanillin and diaminoethane.
L^7 = 2-hydroxybenzyl(2-(pyridin-2-yl)ethylamine.
L^8 = 2-hydroxybenzyl(2-(pyridin-2-yl)methylamine).
Buobb = 1,3-bis(1-butylbenzimidazol-2-yl)-2-oxopropane.
pic = 2,4,6-trinitrophenol.
L^9 = 1,8-[bis(3-formyl-2-hydroxy-5-methyl)benzyl]-l,4,8,11-tetraazacyclotetradecane.
L^{10} = 1,8-[bis(3-formyl-2-hydroxy-5-bromo)benzyl]-l,4,8,11-tetraazacyclotetradecane.

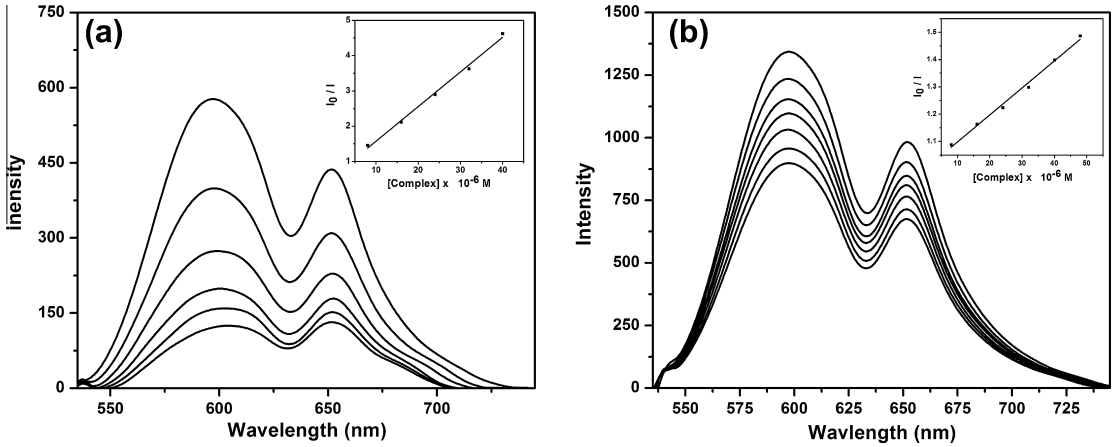

Fig. 6. Emission spectra of EB bound to DNA in the presence of complexes**1** (a) and **2** (b) ([EB] = 3.3 μM, [DNA] = 40 μM, [complex] = 0–25 μM, λ_{ex} = 510 nm). Inset shows the plots of emission intensity I_0/I versus [DNA]/[complex].

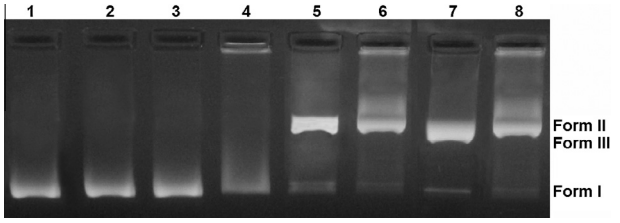

Fig. 7. Cleavage of SC pBR322 DNA (0.2 μg, 33.3 μM) by Cu(II) complexes **1**&**2** in the presence of the reducing agent MPA (0.71 mM) in 50 mM Tris–HCl/50 mM NaCl buffer (pH 7.2). Lane 1, DNA control; lane 2, DNA + MPA; lanes 3&4 DNA + **1**&**2**(200 μM) respectively; lanes 5&6, DNA + MPA + **1**&**2**(100 μM) respectively; lanes 7&8, DNA + MPA + **1**&**2** (200 μM) respectively.

mercaptopropionic acid has a significant effect on DNA cleavage due to formation of reduced copper ions which is more remarkable for **1** where the linear form is observed in large extent. As evident from the literature, complexes of polyamine ligands and the number of chelating metal atoms play an important role due to their good nuclease activity [45]. The cleavage ability of the complexes might be due to the binding affinity of the complex to the DNA, can almost promote the probability of double strand scission once the DNA has undergone a single strand break [15]. Therefore, we conclude that both the complexes show nuclease activity in the presence of reducing agent due to the enhanced stabilization of the Cu(I) species, as evidenced by the highest Cu(II)/Cu(I) redox potential and it is clear that the cleavage of pBR322 DNA is highly dependent on the number of copper ions as well as the presence of an aromatic moiety in the complexes [46–48].

The cleavage mechanism of pBR322 DNA induced by complexes **1**&**2** was investigated (Fig. 8(a) and (b)) and clarified in the presence of singlet oxygen quenchers [49] sodium azide and L-histidine, and hydroxyl radical scavengers [50] DMSO and KI. It is remarkable from Fig. 8(a) that DMSO (lanes 3 and 4) and KI (lanes 6 and 7) are completely ineffective, and these results rule out the possibility of DNA cleavage by hydroxyl radicals. Fig. 8(b) shows that the complexes **1**&**2** exhibits reduced DNA damage in

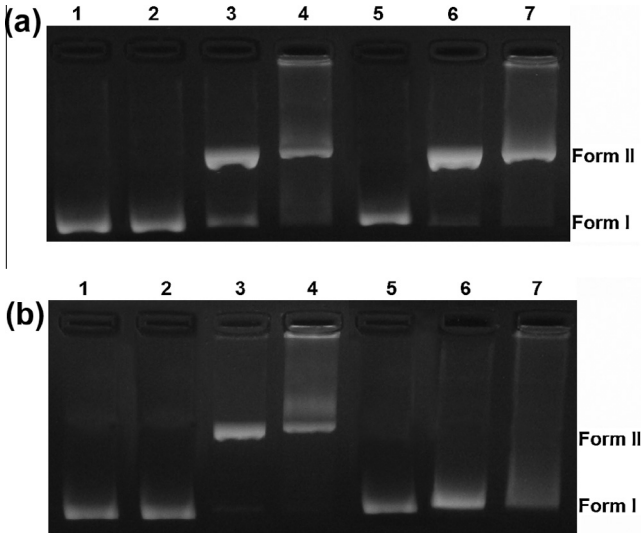

Fig. 8. Cleavage of SC pBR322 DNA (0.2 μg, 33.3 μM) by Cu(II) complexes **1**&**2**(100 μM) in the presence of the reducing agent MPA (0.71 mM) in 50 mM Tris–HCl/50 mM NaCl buffer (pH 7.2). (a) Lane 1, DNA control; lane 2, DNA + MPA + DMSO; lanes 3&4, DNA + MPA + DMSO + **1**&**2**(100 μM) respectively; lanes 5, DNA + MPA + KI; lanes 6&7, DNA + MPA + KI + **1**&**2**(100 μM) respectively. (b) Lane 1, DNA control; lane 2, DNA + MPA + NaN_3; lanes 3&4, DNA + MPA + NaN_3 + **1**&**2**(100 - μM) respectively; lane 5, DNA + MPA + L-histidine; lanes 6&7, DNA + MPA + L-histidine + **1**&**2**(100 μM) respectively.

Table 5
Antibacterial activities of Ligands and its complexes.

Compound	Zone inhibition diameter (mm)			
	Gram negative bacterium		Gram positive bacterium	
	E. coli	Psuedomonas	*B. subtlis*	*S. aureus*
L^1	7	2	7	6
L^2	8	5	10	9
$[CuL^1](ClO_4)_2$	12	9	20	21
$[CuL^2](ClO_4)_2$	18	10	22	25

presence of singlet oxygen quencher sodium azide (lanes 3 and 4) and do not exhibit DNA damage activity in the presence of singlet oxygen quencher L-histidine (lanes 6 and 7). These observations suggest that complexes **1**&**2** mediated cleavage reactions proceed via an oxidative pathway mechanism and imply that singlet oxygen plays a vital role in the cleavage chemistry. In the presence of MPA, the Cu(II) complexes **1**&**2** remarkably degrade pBR322 DNA by an oxidative (O_2-dependent pathway) cleavage mechanism using singlet oxygen as the reactive species [51]. The complex **2** shows better chemical nuclease activity than complex **1**. The structure of the ligand plays an important role in the cleavage [52] which shows a better DNA cleavage ability after combining to the metal ions, so a synergistic effect might exist in the system.

Antibacterial activity

The inhibition efficiencies of the Schiff's base ligands and their copper(II) complexes were tested against two gram positive (*S. aureus*, *Bacillus subtilis*) and two gram negative bacterium (*E. coli* and *P. aeruginosa*). The DMSO used as solvent was kept as control in all plates does not show any zone of inhibition which implies that the solvent not interferes in the antimicrobial activity for the tested microorganisms. The experimental result shown in Table 5 indicates that, both the complexes are having higher inhibition efficiency than their free ligands which can be explained on the basis of chelate formation. When the antimicrobial activity of metal complexes are investigated, the following factors [53–55] should be considered: (i) the chelate effect of ligands; (ii) the nature of the N-donar ligands; (iii) the total charge of the complex; (iv) existence and the nature of the ion neutralizing the ionic complex and (v) the nuclearity of the metal centre in the complex. The chelation reduces the polarity of ligand due to the overlap of the ligand orbital and partial sharing of the positive charge of the copper ion with donor groups. Further, it increases the delocalization of π-electrons over the whole chelate ring and enhances the lipophilic nature of the complexes. This increased lipophilicity enhances the transportation of the complexes into lipid membrane and restricts further multiplicity of the microorganisms. The variation in the effectiveness of different compounds against different organisms depends either on the impermeability of the cells of the microbes or on differences in ribosome of microbial cells. On comparing the gram negative and positive bacterium, the complexes exhibit higher efficiency for gram positive bacterium than that of gram negative bacterium. Thus the synergistic effect of copper ion and counter ions induces the copper(II) complexes to have comparatively greater inhibition than that of their respective free ligands.

Conclusions

In this study, we have synthesized and characterised two mononuclear Cu(II) complexes using Schiff's base ligands and studied their antibacterial activity, DNA binding and cleavage activity. The single crystals X-ray study confirms the structure of ligands

L^1 and L^2. The spectral and structural data evidences for proposed coordination behaviour and geometries of the synthesized Schiff's base copper(II) complexes. The electrochemical study reveals that one electron reduction transfer occurs for both mononuclear complexes. The copper ion in the mononuclear copper complexes has been translocated between two non-equivalent coordinating compartments of a ditopic ligand by varying the pH of the complex solution. The copper(II) complexes show efficient DNA binding ability and the binding constant values of both complexes are in the order of **2** > **1** which show good DNA binding propensity. The DNA cleavage studies for synthesised complexes **1**&**2** in the presence of mercatopropionic acid showed the DNA to be cleaved through an oxidative (O_2-dependent pathway) cleavage mechanism using singlet oxygen as the reactive species, because L-histidine and azide ions were obviously inhibiting the cleavage activity. All the copper(II) complexes show good antimicrobial activity due to synergetic effect of copper atom and the complexes give greater zone of inhibition for gram positive bacterium than that of gram negative bacterium.

Acknowledgements

The authors gratefully acknowledge the financial support of this work by the Department of Science and Technology, New Delhi (DST-SR/FT/CS-049/2009). The authors thank the SAIF Central Drug Research Institute (CDRI), Lucknow for analyzing the mass spectra.

Appendix Supplementary. material

Crystallographic data in CIF format for compound L^1 and L^2 have been deposited at the Cambridge Crystallographic Data Centre, CCDC Nos. 848543 and 886285 respectively. Copies of CIFs are available free of charge from The Director, CCDC, 12 Union Road, Cambridge, CB2 1EZ, UK (Fax: +44 1223 336 033; email: deposit@ccdc.cam.ac.uk or http://www.ccdc.cam.ac.uk). The CIF format of L^1 and L^2 were given in the supplementary material. The mass spectrum of complex **1** was given in the supplementary material. Supplementary data associated with this article can be found, in the online version, at http://dx.doi.org/10.1016/j.saa.2013.11.079.

References

[1] T.D. Tullius, J.A. Greenbaum, Curr. Opin. Chem. Biol. 9 (2005) 127–134.
[2] E. Boseggia, M. Gatos, L. Lucatello, F. Manein, S. Moro, M. Palumbo, C. Sissi, P. Tecilla, U. Tonellato, G.J. Zagotto, Am. Chem. Soc. 126 (2004) 4543–4549.
[3] H.T. Chifotides, K.R. Dunbar, Acc. Chem. Res. 38 (2005) 146–156.
[4] J. Tan, B. Wang, L. Zhu, Bioorg. Med. Chem. Lett. 17 (2007) 1197–1199.
[5] G.J. Chen, X. Qiao, P.Q. Qiao, G.J. Xu, J.Y. Xu, J.L. Tian, W. Gu, X. Liu, S.P. Yan, J. Inorg. Biochem. 105 (2011) 119–126.
[6] D.K. Chand, H.J. Schneider, A. Bencini, A. Bianchi, C. Giorgi, S. Ciattini, B. Valtancoli, Chem. Eur. J. 6 (2000) 4001–4008.
[7] S. Dhar, P.A. Reddy, M. Netaji, S. Mahadevan, M.K. Saha, A.R. Chakravarty, Inorg. Chem. 41 (2002) 3469–3476.
[8] S.Y. Tsang, S.C. Tam, I. Bremner, M.J. Burkitt, Biochem. J. 317 (1996) 13–16.
[9] F.B. Tamboura, M. Gaye, A.H. Barry, T. Jouini, Inorg. Chem. Commun. 5 (2002) 235–238.
[10] P. Kumar, B. Baidya, S.K. Chaturvedi, R.H. Khan, D. Manna, D.B. Mondal, Inorg. Chim. Acta 376 (2011) 264–270.
[11] R. Karmakar, C.R. Choudhary, S. Mitral, L. Dahlenburg, Struct. Chem. 16 (2005) 611–618.
[12] R. Pradhan, A.M. Thomas, A. Mukherjee, S. Dhar, M. Netaji, A.R. Chakravarty, Indian J. Chem. Sec. A 44 (2005) 18–26.
[13] P.K. Sasmal, A.S. Patra, M. Netaji, A.R. Chakravarty, Inorg. Chem. 46 (2007) 11112–11132.
[14] M.Z. Wang, Z.X. Meng, B.L. Liu, G.L. Cai, C.L. Zhang, X.Y. Wang, Inorg. Chem. Commun. 8 (2005) 368–371.
[15] S. Anbu, M. Kandaswamy, Polyhedron 30 (2011) 123–131.
[16] R.B. Xu, X.Y. Xu, J. Zhou, X.J. Wang, W.X. Ma, D.Q. Wang, Y.P. Huang, C.M. Xu, J. Chem. Crystallogr. 41 (2011) 1190–1196.
[17] M. Shamsuddin, A.M. Nur, B.M. Yamin, Acta Crystallogr. 61 (2005) 2263–2264.
[18] M. Thirumavalavan, P. Akilan, M. Kandaswamy, Inorg. Chem. 42 (2003) 3308–3317.
[19] K.R. Adam, G. Anderegg, L.F. Lindoy, H.C. Lip, M. Mcpartlin, J.H. Rea, R.J. Smith, P.A. Tasker, Inorg. Chem. 19 (1980) 2956–2964.
[20] B. Dede, I. Ozmen, F. Karipcin, Polyhedron 28 (2009) 3967–3974.
[21] W.J. Geary, Coord. Chem. Rev. 7 (1971) 81–122.
[22] H. Felora, R. Saeedi, A.H. Mona, A. Payam, N. Bernhard, Polyhedron 31 (2012) 443–450.
[23] A. Sreekanth, M.R.P. Kurup, Polyhedron 22 (2003) 3321–3332.
[24] J.P. Costes, F. Dahan, J.P. Laurent, M. Drillon, Inorg. Chim. Acta 294 (1999) 8–13.
[25] A. Bencini, C. Benelli, D. Gatteschi, C. Zanchini, A.C. Fabretti, G.C. Franchini, Inorg. Chim. Acta 86 (1984) 169–172.
[26] S.K. Mandal, L.K. Thompson, K. Nag, J.P. Charland, K.J. Gabe, J. Inorg. Chem. 26 (1987) 1391–1395.
[27] H. Okawa, M.T. Tadokoro, T.Y. Aretake, M. Ohba, K. Shindo, M. Mitsumi, M. Koikawa, M. Tomono, D.E. Fenton, Dalton Trans. (1993) 253–258.
[28] F. Abba, G.D. Santis, L. Fabbrizzi, M. Licchelli, A.M.M. Lanfredi, P. Pallavicini, A. Poggi, F. Ugozzoli, Inorg. Chem. 33 (1994) 1366–1375.
[29] D.C. Olson, J. Vasilevskis, J. Inorg. Chem. 8 (1969) 1611–1621.
[30] J.M. Chen, W. Wei, W.X.L. Feng, T.B. Lu, Chem. Asian J. 2 (2007) 710–714.
[31] J.P. Costes, F. Dahan, J.P. Laurent, M. Drillon, Inorg. Chim. Acta 294 (1999) 8–12.
[32] F. Arjmand, F. Sayeed, M.J. Mudassir, Photochem. Photobiol. B: Biol. 103 (2011) 166–179.
[33] B. Peng, H. Chao, B. Sun, H. Li, F. Gao, L.N. Ji, Inorg. Biochem. 100 (2006) 1487–1494.
[34] K. Pothiraj, T. Baskaran, N.J. Raman, Coord. Chem. 65 (2012) 2110–2126.
[35] Y. Mei, J.J. Zhou, Z.Q. Pan, J. Coord. Chem. 65 (2012) 643–654.
[36] S.H. Cui, M. Jiang, Y.T. Li, Z.Y. Wu, X.W. Li, J. Coord. Chem. 64 (2011) 4209–4224.
[37] H. Wu, F. Kou, F. Jia, B. Liu, J. Yuan, Y. Bai, Bioinorg. Chem. Appl. 2011 (2011) 1–8.
[38] R. Prabu, A. Vijayaraj, R. Suresh, L. Jagadish, V. Kaviyarasan, V. Narayanan, Bull. Korean Chem. Soc. 32 (2011) 1669–1678.
[39] E.J. Gao, L. Wang, M.C. Zhu, L. Liu, W.Z. Zhang, Eur. J. Med. Chem. 45 (2010) 311–316.
[40] N. Raman, K. Pothiraj, T. Baskaran, J. Coord. Chem. 64 (2011) 3900–3917.
[41] M. Shakira, S. Khanam, M. Azam, M. Aatif, F.J. Firdaus, Coord. Chem. 64 (2011) 3158–3168.
[42] E. Nyarko, N. Hanada, A. Habib, M. Tabata, Inorg. Chim. Acta 357 (2004) 739–745.
[43] Y. Zhao, J. Zhu, W. He, Z. Yang, Y. Zhu, Y. Li, J. Zhang, Z. Guo, Chem. Eur. J. 12 (2006) 6621–6629.
[44] W. Qian, F. Gu, L. Gao, S. Feng, D. Yan, D. Liao, P. Cheng, J. Chem. Soc., Dalton Trans. (2007) 1060–1066.
[45] J.K. Barton, A.C. Raphael, J. Am. Chem. Soc. 106 (1984) 2466–2472.
[46] S. Gama, F. Mendes, F. Marques, I.C. Santos, M.F. Carvalho, I. Correia, J.C. Pessoa, I. Santos, A. Paulo, J. Inorg. Biochem. 105 (2011) 637–644.
[47] M. Tanaka, K. Ohkubo, S. Fukuzumi, J. Phys. Chem. 110 (2006) 11214–11218.
[48] S. Roy, A.K. Dhar, S. Patra, A.R. Chakravarty, Inorg. Chem. 47 (2008) 5625–5633.
[49] K. Sasmal, A.K. Patra, A.R. Chakravarty, J. Inorg. Biochem. 102 (2008) 1463–1472.
[50] Q.L. Zhang, J.G. Liu, H. Chao, G.Q. Xue, L.N. Ji, J. Inorg. Biochem. 83 (2001) 49–56.
[51] H. Kishikawa, Y.P. Jiang, J. Goodisman, J.C. Dabrowiak, J. Am. Chem. Soc. 113 (1991) 5434–5438.
[52] J.A. Cowan, C. Opin, Chem. Biol. 5 (2001) 634–640.
[53] N. Grover, N. Gupta, P. Singh, H.H. Thorp, Inorg. Chem. 31 (1992) 2014–2023.
[54] C.T. Yang, B. Moubaraki, K.S. Murray, J.J. Vittal, Dalton Trans. (2003) 880–889.
[55] C. Dendrinou-Samara, G. Psomas, C.P. Raptopoulou, D.P. Kessissoglou, J. Inorg. Biochem. 83 (2001) 7–16.